Application of Grey Wolf Optimizer Algorithm for Optimal Power Flow of Two-Terminal HVDC Transmission System

Heba Ahmed HASSAN[1], *Mohamed ZELLAGUI*[2]

[1]Electrical Power and Machines Department, Faculty of Engineering, Cairo University, Cairo University Street, 12613 Giza, Egypt
[2]Electrical Engineering Department, Faculty of Technology, University of Batna 2, Fesdis, 53 Batna, Algeria

hebahassan@ieee.org, m.zellagui@univ-batna2.dz

DOI: 10.15598/aeee.v15i5.2110

Abstract. *This paper applies a relatively new optimization method, the Grey Wolf Optimizer (GWO) algorithm for Optimal Power Flow (OPF) of two-terminal High Voltage Direct Current (HVDC) electrical power system. The OPF problem of pure AC power systems considers the minimization of total costs under equality and inequality constraints. Hence, the OPF problem of integrated AC-DC power systems is extended to incorporate HVDC links, while taking into consideration the power transfer control characteristics using a GWO algorithm. This algorithm is inspired by the hunting behavior and social leadership of grey wolves in nature. The proposed algorithm is applied to two different case-studies: the modified 5-bus and WSCC 9-bus test systems. The validity of the proposed algorithm is demonstrated by comparing the obtained results with those reported in literature using other optimization techniques. Analysis of the obtained results show that the proposed GWO algorithm is able to achieve shorter CPU time, as well as minimized total cost when compared with already existing optimization techniques. This conclusion proves the efficiency of the GWO algorithm.*

Keywords

Grey Wolf Optimizer (GWO) algorithm, High Voltage Direct Current (HVDC), intelligent power systems, Optimal Power Flow (OPF), optimization methods.

1. Introduction

In a High Voltage Direct Current (HVDC) transmission system, an inverter station converts the AC electrical power into DC. After transmission, a rectifier converts the DC electrical power back to AC. These converters can be located in one place as a back-to-back HVDC system, or electrical power can be transmitted from one converter station to another over long distance via an overhead transmission line or an underground cable [1]. HVDC systems serve as ideal supplements to existing AC power networks. The advantages of using HVDC systems include providing economical and more efficient transmission of electrical power over long distances, solving synchronism-related problems by connecting asynchronous networks or networks which operate at different frequencies, providing controlled power supply in either direction and offering access for onshore and offshore power generation from renewable energy sources [2].

As reported in literature, the first commercial application of HVDC transmission took place between the Swedish mainland and the island of Gotland in 1954, using mercury-arc valves. The first 320 MW, thyristor-based HVDC system was commissioned in 1972 between Canadian provinces of New-Brunswick and Quebec [3]. The converters used for HVDC systems are grouped into these categories: line-commutated converters and voltage-source converters or current-source converters. In AC power systems, the Optimal Power Flow (OPF) problem is defined by nonlinear, non-convex equations.

Feasibility studies are required to determine preliminary parameters of the planned system modifications. To incorporate results of power flow and other parame-

ters, more detailed studies are needed. Finally, operating studies are necessary to successfully integrate the HVDC facility into the power system [4]. In HVDC systems, where no reactive power is involved, the OPF problem is less complex but it still retains its nonlinear characteristic when voltage control and optimal storage operation are included in the formulation. There are several different methods solving the resulting nonlinear equations [5].

More recently, some authors have proposed other methods to solve this problem. Authors in [6] and [7] present the model of a voltage-source converter suitable for OPF solution of HVDC using Newton Raphson Algorithm (NRA) and a sequential method was introduced [8]. A new approach for load flow analysis of integrated HVDC power systems using sequential modified Gauss-Seidel method was reported [9]. In [10], a multi-terminal HVDC power flow with a conventional AC power flow has been proposed. In [11], a steady-state multi-terminal HVDC model for power flow has been developed and it includes converter limits, as well as different converter topologies. Other authors have solved this problem by applying new techniques, such as Artificial Bee Colony (ABC) algorithm [12], Genetic Algorithm (GA) [13] and Backtracking Search Algorithm (BSA) [14]. Authors in [15] proposed an OPF in order to minimize the losses in a multi-terminal HVDC grid. Application of transient stability constraints for OPF, to a transmission system including an HVDC, was proposed [16]. Authors in [17] applied an information gap decision theory to the OPF model for the optimal operation of AC-DC systems with offshore wind farms.

In the last two years, Grey Wolf Optimizer (GWO) algorithm has been applied in power systems for solving combined economic emission dispatch problems [18], studying the blackout risk prevention in a smart grid based flexible optimal strategy [19] and estimating the parameters of the Proportional Integral (PI) controller for automatic generation control of two-area power system [20]. Furthermore, it has been used for optimizing wide-area power system stabilizer design [21], solving OPF problem [22] and [23], load frequency control of interconnected power system [24] and economic dispatch problems [25]. It has been also used for solving the optimizing PID controller for automatic generation control of a multi-area thermal power system [26] and the design of Static Synchronous Series Compensator (SSSC) based stabilizer to damp inter-area oscillations [27].

In this paper, the GWO algorithm is used to achieve OPF of the two-terminal HVDC system. The proposed algorithm is applied to two different case-studies which are: the modified 5-bus and WSCC 9-bus test systems. The validity and efficiency of the proposed algorithm are evaluated by comparing the obtained results with those obtained when applying other methods reported in literature such as Backtracking Search Algorithm (BSA) [14], Artificial Bee Colony (ABC) algorithm [12], Genetic Algorithm (GA) [13] and Newton-Raphson Method (NRM) [7].

2. Two-Terminal HVDC Modeling

A basic schematic diagram of a two-terminal HVDC transmission link is given in Fig. 1.

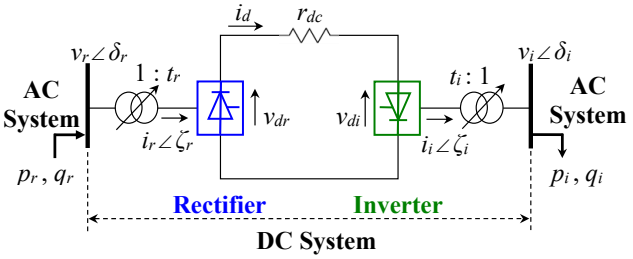

Fig. 1: A basic schematic diagram of a two-terminal HVDC transmission link.

In Fig. 1, v_r and v_i are the AC voltages (rms) at the converter transformer primary, i_r and i_i are the currents at the AC sides of the rectifier and inverter. δ_r and δ_i are the bus voltage phase angles, ξ_r and ξ_i are the current angles and r_{dc} is DC link resistance. p_r and p_i are the active powers at the rectifier and inverter sides, q_r and q_i are the reactive powers at the rectifier and inverter sides and i_d is the direct current of HVDC link. The basic converter equations between AC and DC sides for the rectifier terminal are expressed as follows [7], [12], [13] and [14]:

$$v_{dor} = k \cdot t_r \cdot v_r, \tag{1}$$

$$v_{dr} = v_{dor} \cos\alpha - r_{cr} \cdot i_d, \tag{2}$$

$$p_r = v_{dr} \cdot i_d, \tag{3}$$

$$\phi_r = \cos^{-1}\left(\frac{v_{dr}}{v_{dor}}\right), \tag{4}$$

$$q_r = |p_r \cdot \tan\phi_r|, \tag{5}$$

where the constant k is equal to $3\sqrt{2}/\pi$, v_{dor} is the open circuit DC voltage at the rectifier side; r_{cr} is the equivalent commutation resistance at the rectifier side and equal to $\sqrt{3}x_{cr}/\pi$ (x_{cr} is the equivalent commutation reactance at the rectifier side), and $\phi_r = \delta_r - \xi_r$ is the phase angle between the AC voltage and the fundamental AC current at the rectifier side.

The basic converter equations between AC and DC sides for the inverter terminal are also expressed as follows [7], [12], [13] and [14]:

$$v_{doi} = k \cdot t_i \cdot v_i, \tag{6}$$

$$v_{di} = v_{doi} \cos\gamma - r_{ci} \cdot i_d, \tag{7}$$

$$p_i = v_{di} \cdot i_d, \tag{8}$$

$$\phi_i = \cos^{-1}\left(\frac{v_{di}}{v_{doi}}\right), \tag{9}$$

$$q_i = |p_i \cdot \tan\phi_i|, \tag{10}$$

where v_{doi} is the open circuit dc voltage at the inverter side; r_{ci} is the equivalent commutation resistance at the inverter side, and $\Phi_i = \delta_i - \xi_i$ is the phase angle between the AC voltage and the fundamental AC current at the inverter side. An equivalent circuit of a two-terminal HVDC link is shown in Fig. 2.

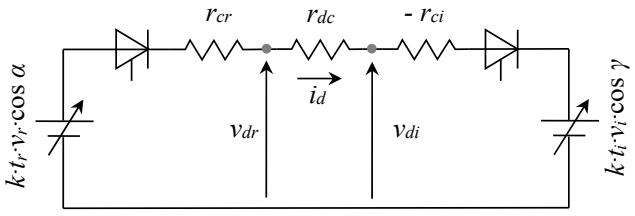

Fig. 2: An equivalent circuit of a two-terminal HVDC link.

In Fig. 2, α is the ignition delay angle, γ is the extinction advance angle, and v_{dr} and v_{di} are the DC link voltages at the rectifier and inverter terminals. The relationship between the rectifier and inverter terminal voltages of the DC link can be expressed by considering DC link resistance as follows:

$$v_{dr} - v_{di} - r_{dc} \cdot i_d = 0. \tag{11}$$

3. Problem Formulation and Constraints

The OPF is an optimization problem whose mathematical equations are expressed as follows:

$$\text{Minimize } f(x,u). \tag{12}$$

$$\text{Subject to: } \begin{cases} g(x,u) = 0, \\ h(x,u) \le 0. \end{cases} \tag{13}$$

The objective function $f(x,u)$ considers the production cost of the entire power system and the equality constraints $g(x,u)$ consider the power flow equations related to the entire power system. The inequality constraints $h(x,u)$ consider the limits of the variables related to the entire power system. The variables $x = (x_1, \ldots, x_n)$ and $u = (u_1, \ldots, u_n)$ of these functions are the state and control vectors, respectively.

3.1. Control Variables

The control variables should be the same as those of the problem to be optimized. The AC and DC system state variables in per unit are selected as follows [12], [13] and [14]:

$$x = [x_{AC}, x_{DC}], \tag{14}$$

$$x_{AC} = [p_{gslack}, q_{g1}, \ldots, q_{gNg}, v_{L1}, \ldots, v_{LNl}], \tag{15}$$

$$x_{DC} = [t_r, t_i, \alpha, \gamma, v_{dr}, v_{di}], \tag{16}$$

where p_{gslack} is the slack bus active power output, q_{gi} is the reactive power outputs, v_{Li} is the load bus voltage magnitudes, and N_l is the number of load buses. The AC and DC system control variables in per unit are also selected as follows [12], [13] and [14]:

$$u = [u_{AC}, u_{DC}], \tag{17}$$

$$u_{AC} = [p_{g2}, \ldots, p_{gNg}, v_{g1}, \ldots, v_{gNg}, t_1, \ldots, t_{N_T}], \tag{18}$$

$$u_{DC} = [p_r, p_i, q_r, q_i, d_i], \tag{19}$$

where p_{gi} (except for the slack bus p_{gslack}) is the generator active power outputs, v_{gi} is the generator voltage magnitudes, N_g is the number of the generator buses, t_i is the transformer tap ratios, N_T is the number of transformers, p_r and p_i are the active powers at the rectifier and inverter sides, q_r and q_i are the reactive powers at the rectifier and inverter sides, and i_d is the direct current of HVDC link.

3.2. Objective Function

The problem is minimization of the total production cost (F_{cost}) in a power system. In other words, the aim is minimization of objective function which is power loss in an energy system. At the same time, the objective function of whole system is minimized under equality and inequality constraints. Therefore, the objective function (f) can be as follows:

$$f(x,u) = F_{\cos t} = \sum_{i=1}^{N_g} \left(a_i \cdot p_{gi}^2 + b_i \cdot p_{gi} + c_i\right), \tag{20}$$

where F_{cost} represents the total production cost; a_i, b_i and c_i represent the production cost coefficients of the i^{th} generator.

3.3. Equality Constraints

1) AC System Equality Constraints

A representation of the AC bus connected to the DC transmission link is shown in Fig. 3. The equalities related to the k^{th} bus are given by:

$$p_{gk} - p_{lk} - p_{dk} - p_k = 0, \tag{21}$$

$$q_{gk} + q_{sk} - q_{lk} - q_{dk} - q_k = 0. \tag{22}$$

In Fig. 3, p, q, v and δ represent the active power, reactive power, bus voltage magnitudes, and bus voltage angles, respectively. The subscripts g, l, s and d represent generator, load, shunt reactive compensator, and DC link, respectively.

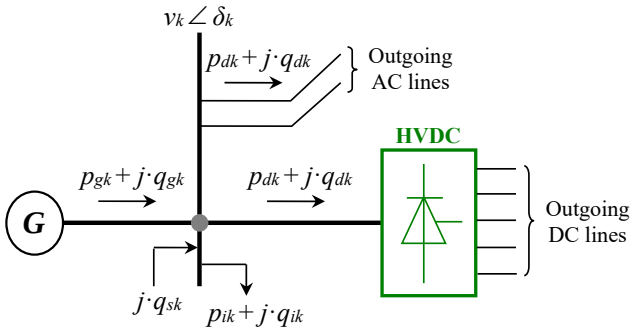

Fig. 3: Representation of AC bus connected to HVDC transmission link [7].

The active and reactive powers transferred from the k^{th} bus to the AC line are also expressed as:

$$p_k = v_k \sum_{j=1}^{N} v_j \left(G_{kj} \cos \delta_{kj} + B_{kj} \sin \delta_{kj}\right), \tag{23}$$

$$q_k = v_k \sum_{j=1}^{N} v_j \left(G_{kj} \sin \delta_{kj} - B_{kj} \cos \delta_{kj}\right), \tag{24}$$

where v_j and v_k are the voltage magnitudes of the j^{th} and k^{th} buses; G_{kj} and B_{kj} are the transfer conductance and susceptance between buses k and j of the bus admittance matrix Y_{bus}. δ_{kj} is the voltage phase angle difference between buses k and j and N is the number of buses in the power system.

2) DC System Equality Constraints

By neglecting the converter and transformer losses in the power system, the power of the rectifier bus becomes equal to that of the inverter bus. Hence, the equations that represent the equality constraints of the DC system are:

$$p_{dk} = p_r, \tag{25}$$

$$q_{dk} = q_r, \tag{26}$$

$$p_{dk} = -p_i, \tag{27}$$

$$q_{dk} = q_i. \tag{28}$$

3.4. Generation Capacity Constraints

For stable operation, the values of the generator active and reactive power outputs, bus voltage magnitudes, transformer tap ratios and shunt VAR compensation are restricted by their lower and upper limits as follows [7], [12], [13] and [14]:

$$p_{gi}^{\min} \le p_{gi} \le p_{gi}^{\max} \quad i = 1, \ldots, N_g, \tag{29}$$

$$q_{gi}^{\min} \le q_{gi} \le q_{gi}^{\max} \quad i = 1, \ldots, N_g, \tag{30}$$

$$q_{si}^{\min} \le q_{si} \le q_{si}^{\max} \quad i = 1, \ldots, N_c, \tag{31}$$

$$v_i^{\min} \le v_i \le v_i^{\max} \quad i = 1, \ldots, N, \tag{32}$$

$$t_i^{\min} \le t_i \le t_i^{\max} \quad i = 1, \ldots, N_T, \tag{33}$$

where N_c is the number of the compensation devices.

3.5. DC Transmission Link Constraints

These constraints are represented by the upper and lower limits of the corresponding variables as follows [7], [12], [13] and [14]:

$$p_{dk}^{\min} \le p_{dk} \le p_{dk}^{\max} \quad k = 1, 2, \tag{34}$$

$$q_{dk}^{\min} \le q_{dk} \le q_{dk}^{\max} \quad k = 1, 2, \tag{35}$$

$$t_{dk}^{\min} \le t_{dk} \le t_{dk}^{\max} \quad k = 1, 2, \tag{36}$$

$$v_{dk}^{\min} \le v_{dk} \le v_{dk}^{\max} \quad k = 1, 2, \tag{37}$$

$$i_d^{\min} \le i_d \le i_d^{\max}, \tag{38}$$

$$\alpha^{\min} \le \alpha \le \alpha^{\max}, \tag{39}$$

$$\gamma^{\min} \le \gamma \le \gamma^{\max}. \tag{40}$$

4. Grey Wolf Optimizer (GWO) Algorithm

The Grey Wolf Optimizer (GWO) algorithm mimics the leadership hierarchy and hunting mechanism of grey wolves in nature proposed by Mirjalili et al. in 2014 [28] and [29]. The hunting technique and the social hierarchy of grey wolves are mathematically modeled in order to design GWO and perform optimization.

The mathematical model of the encircling behavior is represented by the following equations [28]:

$$\vec{D} = |\vec{C} \cdot \vec{X}_p(iter) - \vec{X}(iter)|, \tag{41}$$

$$\vec{X}(iter+1) = \vec{X}_p(iter) - \vec{A} \cdot \vec{D}, \tag{42}$$

where $iter$ is the current iteration and $X_{P(iter)}$ represents the position vector of the victim. The $\vec{A}$ and $\vec{C}$ are coefficient vectors which are given by:

$$\begin{cases} \vec{A} = 2 \cdot \vec{a} \cdot \vec{r}_1 - \vec{a}, \\ \vec{C} = 2 \cdot \vec{r}_2. \end{cases} \tag{43}$$

where a is linearly decreased from 2 to 0 over the course of iterations, $\vec{r}_1$ and $\vec{r}_2$ are random vectors in the range of 0 to 1.

In GWO, the first three best solutions obtained are stored so far and push the other search agents to update their positions due to the position of the best search agents. In order to formulate the social hierarchy of wolves when designing GWO algorithm, the population is split into four groups: alpha (α), beta (β), delta (δ) and omega (ω).

Over the course of iterations, the first three best solutions are called α and δ, respectively. Figure 4 shows how to update the locations of α, β and δ, respectively, in a two-dimensional space.

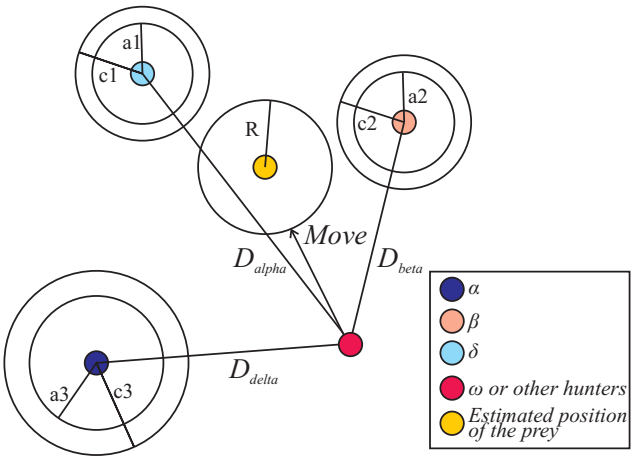

Fig. 4: Position updating in GWO [28].

The rest of the candidate solutions are denoted as ω. In this algorithm, the hunting/optimization is guided by α, β, δ and ω. The wolves are required to encircle α, β and δ to find better solutions [28], [29] and [30].

Save the first three best solutions obtained so far and oblige the other search agents (including the omegas) to update their positions according to the position of the best search agent. The following formulas are proposed in this regard.

$$\vec{D}_\alpha = |\vec{C}_1 \cdot \vec{X}_\alpha - \vec{X}|, \tag{44}$$

$$\vec{D}_\beta = |\vec{C}_2 \cdot \vec{X}_\beta - \vec{X}|, \tag{45}$$

$$\vec{D}_\delta = |\vec{C}_3 \cdot \vec{X}_\delta - \vec{X}|, \tag{46}$$

$$\vec{X}_1 = \vec{X}_\alpha - \vec{A}_1 \cdot (\vec{D}_\alpha), \tag{47}$$

$$\vec{X}_2 = \vec{X}_\beta - \vec{A}_2 \cdot (\vec{D}_\beta), \tag{48}$$

$$\vec{X}_3 = \vec{X}_\delta - \vec{A}_3 \cdot (\vec{D}_\delta), \tag{49}$$

$$\vec{X}(iter+1) = \frac{\vec{X}_1 + \vec{X}_2 + \vec{X}_3}{3}. \tag{50}$$

With these equations, a search agent updates its position according to α, β, δ, in a dimensional search space.

In these formulas, vectors $\vec{A}$ and $\vec{C}$ are obliging the GWO algorithm to explore and exploit the search space. With decreasing $\vec{A}$, half of the iterations is devoted to exploration ($|\vec{A} \geq 1|$) and the other half is dedicated to exploitation ($|\vec{A} < 1|$).

The range of $\vec{C}$ is $2 \leq \vec{C} \leq 0$ and the vector $\vec{C}$ also improves exploration when $\vec{C} > 1$. Exploitation is emphasized when $\vec{C} < 1$; $\vec{A}$ is decreased linearly over the course of the iterations [29] and [30]. In contrast, $\vec{C}$ is generated randomly to emphasize the exploration/exploitation at any stage and to avoid local optima.

5. Simulation Results

To show the applicability and efficiency of the proposed GWO optimization algorithm in solving the OPF problem of a two-terminal HVDC system, we tested it on the two test systems. The parameters used for the proposed GWO algorithm are given by: the population size is 80, the coefficient a is between $[0, 2]$, the random vectors $\vec{r}_1$ and $\vec{r}_2$ belong to interval $[0, 1]$ and the stopping criterion of the algorithm is set as 100 iterations for each of the two test systems. The developed

program using MATLAB is run on a computer with processor Intel-core i3-5010 U, CPU 2.1 GHz, 4 GB RAM.

Figure 5 shows the flow chart of the sequential power flow algorithm now combined in a sequential AC/DC [11] and [31]. Applied the traditional Newton-Raphson method is used for the sequential AC power flow algorithm is the first step and a linear current-balancing method is used for the sequential DC power flow algorithm.

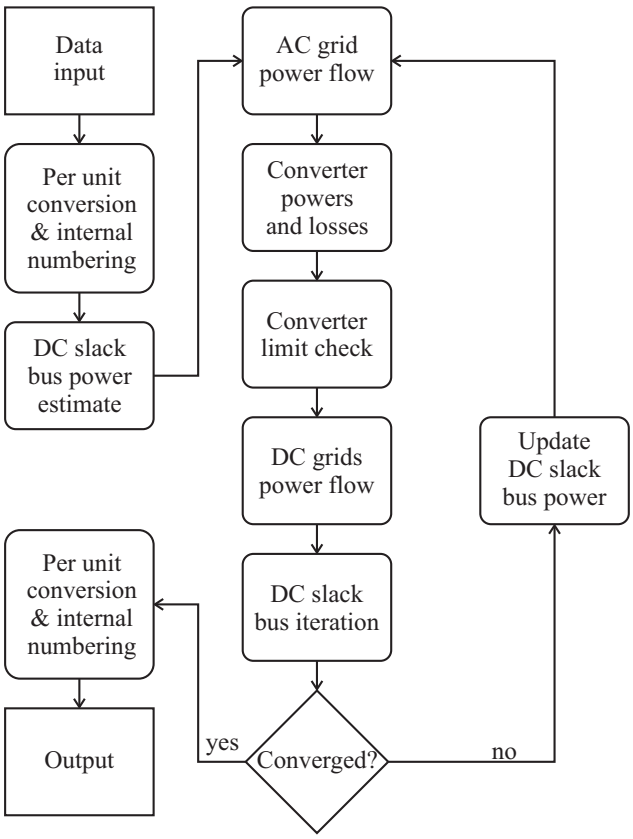

Fig. 5: Flow chart of the sequential VSC AC/DC power flow algorithm [11] and [31].

5.1. First Case-Study: 5-Bus Test System

The system shown in Fig. 6 [7] has five buses and two generators and it is extended with a two-terminal HVDC link. The AC network and HVDC converters are assumed to work under three-phase balanced conditions. The experiment is performed for two different scenarios, according to the power and current of the DC link, which are:

- Scenario A: The current of the DC link is considered to be 0.10 p.u.
- Scenario B: The current of the DC link is considered to be 0.15 p.u.

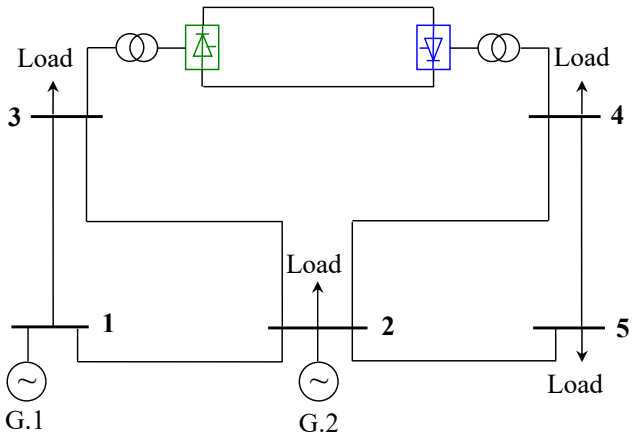

Fig. 6: The 5-bus test system.

The convergence characteristics of the GWO optimization algorithm for the two scenarios of the first case-study are presented in Fig. 7. A lower DC current, as given in Scenario A, encounters less iterations than for Scenario B.

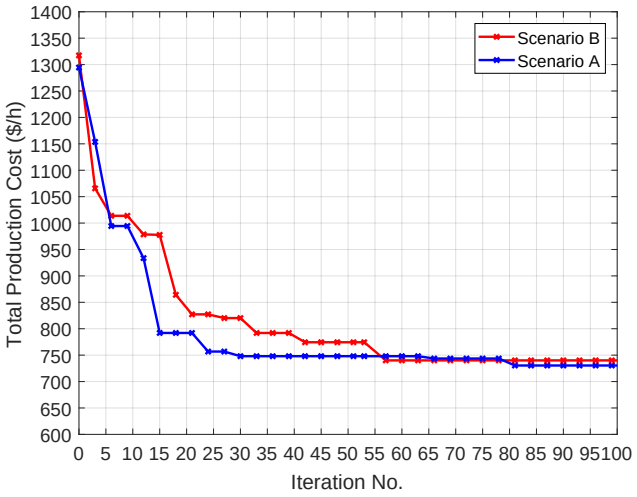

Fig. 7: Convergence curve of the GWO algorithm for the two scenarios of the first case-study.

Table 1 and Tab. 2 represent the simulation results obtained when applying BSA [14], ABC [12], GA [13], NRM [7], and GWO algorithms to the two scenarios of the first case-study.

5.2. Second-Case Study: WSCC 9-Bus Test System

The WSCC 9-bus system shown in Fig. 8 [13] consists of three generators, six transmission line, three power transformers, and three loads connected at buses 5, 6,

Tab. 1: The first case-study (Scenario A): Simulation results obtained for BSA, ABC, GA, NRM and GWO algorithms.

Variable	Limit (p.u.)		BSA	ABC	GA	NRM	GWO
	Min	Max	[14]	[12]	[13]	[7]	
Generator Active Outputs							
p_{g1}	0.10	2.00	0.8000	0.7931	0.7949	0.8013	0.8031
p_{g2}	0.10	2.00	0.8805	0.8873	0.8855	0.8796	0.8701
Generator Reactive Outputs							
q_{g1}	−3.00	3.00	−0.1503	−0.1397	−0.1403	0.2029	−0.1499
q_{g2}	−3.00	3.00	0.0742	0.0863	0.0649	0.0315	0.0743
Nodal Voltages							
v_1	0.90	1.10	1.1000	1.1000	1.0996	1.109	0.9975
v_2	0.90	1.10	1.0950	1.0946	1.0941	1.100	1.0932
v_3	0.90	1.10	1.0692	1.0686	1.0686	1.071	1.0706
v_4	0.90	1.10	1.0781	1.0756	1.0772	1.075	1.0819
v_5	0.90	1.10	1.0727	1.0716	1.0718	1.071	1.0743
DC System							
p_{dr}	0.10	0.15	0.1499	0.1458	0.1493	0.1371	0.1321
p_{di}	0.10	0.15	0.1499	0.1457	0.1492	0.1371	0.1321
q_{dr}	0.0	0.10	0.0279	0.0330	0.0277	0.0230	0.0264
q_{di}	0.0	0.10	0.0407	0.0575	0.0409	0.0389	0.0421
i_d	0.10	0.10	0.1000	0.1000	0.1000	0.1000	0.1000
t_r	0.90	1.10	1.0566	1.03591	1.0525	0.940	1.0532
t_i	0.90	1.10	1.0673	1.0788	1.0640	0.962	1.0701
α (°)	10	20	10.2856	12.5486	10.3995	10.839	10.3481
γ (°)	15	25	15.1004	21.4680	15.2674	16.735	16.0023
v_{di}	1.00	1.50	1.4999	-	-	1.337	1.4037
v_{di}	1.00	1.50	1.4996	-	-	1.336	1.4037

Tab. 2: The first case-study (Scenario B): Simulation results obtained for BSA, ABC, GA, NRM and GWO algorithms.

Variable	Limit (p.u.)		BSA	ABC	GA	NRM	GWO
	Min	Max	[14]	[12]	[13]	[7]	
Generator Active Outputs							
p_{g1}	0.10	2.00	0.8012	0.7979	0.8101	-	0.7099
p_{g2}	0.10	2.00	0.8795	0.8828	0.8708	-	0.8711
Generator Reactive Outputs							
q_{g1}	−3.00	3.00	−0.1376	−0.2426	−0.1889	-	−0.1353
q_{g2}	−3.00	3.00	0.0903	0.1882	0.1426	-	0.0916
Nodal Voltages							
v_1	0.90	1.10	1.1000	1.1000	1.0994	-	1.1000
v_2	0.90	1.10	1.0949	1.1000	1.0967	-	1.0951
v_3	0.90	1.10	1.0667	1.0697	1.0674	-	1.0732
v_4	0.90	1.10	1.0775	1.0832	1.0795	-	1.0942
v_5	0.90	1.10	1.0725	1.0779	1.0744	-	1.0819
DC System							
p_{dr}	0.15	0.225	0.1913	0.1928	0.1941	0.1945	0.1956
p_{di}	0.15	0.225	0.1912	0.1927	0.1940	0.1944	0.1941
q_{dr}	0.0	0.10	0.0360	0.0363	0.0370	0.0443	0.0387
q_{di}	0.0	0.10	0.0603	0.0571	0.0611	0.0588	0.0672
i_d	0.15	0.15	0.1500	0.1500	0.1500	0.1500	0.1500
t_r	0.90	1.10	0.9009	0.9055	0.9138	-	0.9051
t_i	0.90	1.10	0.9187	0.9161	0.9302	-	0.9281
α (°)	10	20	10.2160	10.2463	10.5539	-	10.1147
γ (°)	15	25	17.3566	16.3448	17.4056	-	16.3271
v_{di}	1.00	1.50	1.2754	-	-	-	1.2644
v_{di}	1.00	1.50	1.2749	-	-	-	1.2681

and 8, of 315 MW active loads and 115 MVAR reactive loads. It is extended with a two-terminal HVDC link which replaces the AC line between buses 4 and 5 in the original WSCC 9-bus test system.

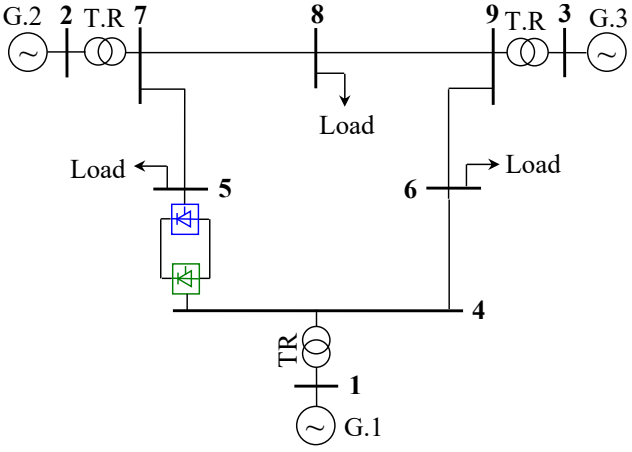

Fig. 8: The WSCC 9-bus test system.

The convergence characteristics of the GWO optimization algorithm for the second case-study are presented in Fig. 9.

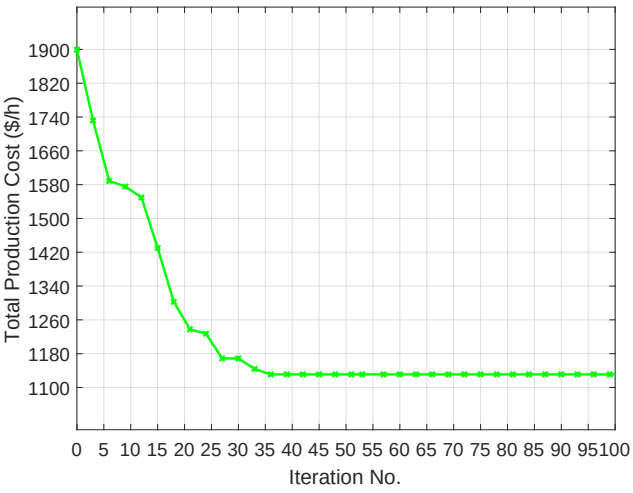

Fig. 9: Convergence curve of the GWO algorithm for the second case-study.

Table 3 represents the simulation results obtained when applying BSA [14], GA [13], and GWO algorithms to the second case-study.

Tab. 3: The second case-study: Simulation results obtained for BSA, GA and GWO algorithms.

Variable	Limit (p.u.)		BSA [14]	GA [13]	GWO
	Min	Max			
Generator Active Outputs					
p_{g1}	0.10	2.00	0.8012	0.7979	0.8113
p_{g2}	0.10	3.00	1.1323	1.2250	1.1397
p_{g3}	0.10	2.70	0.9872	1.0294	0.9721
Generator Reactive Outputs					
q_{g1}	−3.00	3.00	0.2076	0.0109	0.2130
q_{g2}	−3.00	3.00	0.5808	0.7018	0.5812
q_{g3}	−3.00	3.00	−0.1043	−0.1352	−0.1123
Nodal Voltages					
v_1	0.90	1.10	0.9410	1.0636	0.9386
v_2	0.90	1.10	1.0100	1.0839	1.0422
v_3	0.90	1.10	1.0120	1.0612	1.1350
v_4	0.90	1.10	1.0360	1.0474	1.0375
v_5	0.90	1.10	0.9190	0.9248	0.9211
v_6	0.90	1.10	1.0250	1.0344	1.0146
v_7	0.90	1.10	1.0370	1.0479	1.0274
v_8	0.90	1.10	1.0280	1.0345	1.0321
v_9	0.90	1.10	1.0450	1.0469	1.3452
t_{14}	0.85	1.15	0.9000	1.0161	0.9153
t_{27}	0.85	1.15	0.9451	0.9981	0.9374
t_{39}	0.85	1.15	0.9757	1.0227	0.9821
DC System					
p_{dr}	0.1	1.5	0.7107	0.1360	0.7174
p_{di}	0.1	1.5	0.7103	0.1360	0.7124
q_{dr}	0.0	1.0	0.1635	0.0240	0.1702
q_{di}	0.0	1.0	0.1804	0.0266	0.1800
i_d	0.1	1.0	1.2298	0.1000	1.2134
t_r	0.85	1.15	0.9025	0.9765	0.8932
t_i	0.85	1.15	1.0222	1.1097	1.1233
α (°)	7.00	10.00	9.5529	9.4173	9.3922
γ (°)	10.00	15.00	10.8126	10.4741	10.4532
v_{dr}	1.00	1.50	1.2304	-	1.2311
v_{di}	1.0	1.50	1.2298	-	1.2264

Tab. 4: Total costs and CPU times of the first case-study.

	BSA [14]	ABC [12]	GA [13]	NRM [7]	GWO
Year	2016	2013	2014	2008	2017
Scenario A					
Total Cost ($/h)	748.022	748.055	748.152	748.156	747.541
CPU Time (sec)	1.73	1.90	6.76	-	1.32
Scenario B					
Total Cost ($/h)	748.092	748.151	748.282	748.451	747.932
CPU Time (sec)	1.76	1.94	6.69	-	1.33

5.3. Comparative Study

Table 4 and Tab. 5 compare the total cost and CPU time for all of the tested techniques in the first and second case-study, respectively.

When using various optimization algorithms including GWO, the comparative costs and CPU times of the two case-studies are represented in Fig. 10, and Fig. 11, respectively.

As shown in Fig. 10, the cost encountered by applying the proposed GWO algorithm is lower than that obtained when applying the BSA, ABC, GA, or NRM algorithm for the first case-study. This observation is still valid for the second case-study when comparing

Tab. 5: Total costs and CPU times of the second case-study.

	BSA [14]	**GA** [13]	**GWO**
Year	2016	2014	2017
Total Cost ($/h)	1135.032	1145.952	1129.470
CPU Time (sec)	5.15	47.44	4.23

the cost of applying the GWO algorithm with that of applying BSA or GA algorithm.

According to Fig. 11, applying the proposed GWO algorithm attracts the lowest CPU time when compared with other optimization algorithms for the two cases studied in this paper.

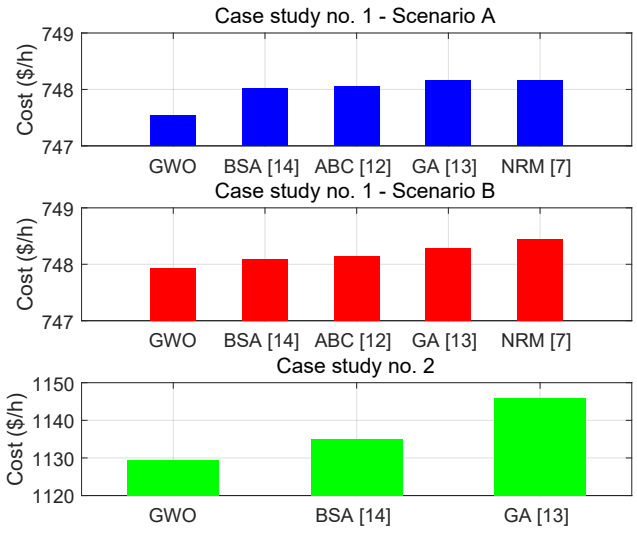

Fig. 10: Estimated costs of the two case-studies.

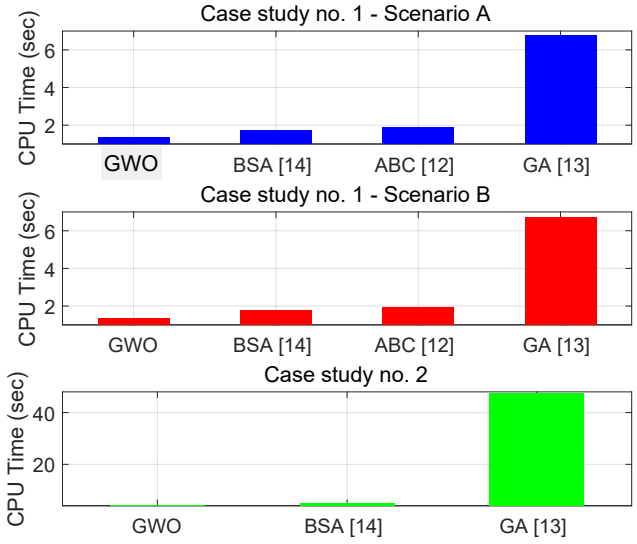

Fig. 11: CPU times of the two case studies.

6. Conclusion

In this paper, the OPF problem of a two-terminal HVDC transmission power system was addressed using the proposed GWO algorithm. The algorithm was applied to two HVDC test systems, namely the 5-bus and the WSCC 9-bus test systems.

The total costs and CPU times encountered when applying the GWO algorithm showed to be lower than those obtained when using other optimization algorithms, such as BSA, ABC, GA, and NRM, with a faster rate of convergence.

The GWO algorithm demonstrated several advantages such as fast convergence, adaptability and reliability to the optimal solution with a performance that was not sensitive to the initial conditions. Therefore, the scope of the future work is to apply the GWO algorithm to solve the OPF problems of large power systems equipped with FACTS devices and renewable energy sources.

References

[1] EREMIA, M., C. C. LIU and A.-A. EDRIS. *Advanced Solutions in Power Systems: HVDC, FACTS, and Artificial Intelligence*. Piscataway: IEEE Press, 2016. ISBN 978-1119035695.

[2] SHARIFABADI, K., L. HARNEFORS, H. P. NEE, S. NORRGA and R. TEODORESCU. *Design, control, and application of modular multilevel converters for HVDC transmission systems*. Chichester: Wiley, 2016. ISBN 978-1-118-85156-2.

[3] SOOD, V. K. *HVDC and FACTS controllers applications of static converters in power systems*. Boston: Kluwer Academic, 2004. ISBN 978-1402078910.

[4] PADIYAR, K. R. *HVDC power transmission systems*. 2nd ed. Tunbridge Wells: New Academic Science, 2011. ISBN 978-1906574772.

[5] CARRIZOSA, M. J., F. D. NAVAS, G. DAMM and F. LAMNABHI-LAGARRIGUE. Optimal Power Flow in Multi-terminal HVDC Grids with Offshore Wind Farms and Storage Devices. *International Journal of Electrical Power and Energy Systems*. 2015, vol. 65, iss. 1, pp. 291–298. ISSN 0142-0615. DOI: 10.1016/j.ijepes.2014.10.016.

[6] PIZANO-MARTINEZ, A., C. R. FUERTE-ESQUIVEL, H. AMBRIZ-PEREZN and E. ACHA. Modeling of VSC-based HVDC Systems for a Newton-Raphson OPF Algorithm. *IEEE Power Systems*. 2007, vol. 22,

iss. 4, pp. 1794–1803. ISSN 0885-8950. DOI: 10.1109/TPWRS.2007.907535.

[7] AMBRIZ-PEREZ, H., E. ACHA and C. R. FUERTE-ESQUIVEL. High Voltage Direct Current Modeling in Optimal Power Flows. *International Journal of Electrical Power & Energy Systems*. 2008, vol. 30, iss. 3, pp. 157–168. ISSN 0142-0615. DOI: 10.1016/j.ijepes.2007.06.010.

[8] LIU, C., A. BOSE and Y. HOU. Discussion of the Solvability of HVDC Systems Power Flow with a Sequential Method. *Electric Power Systems Research*. 2012, vol. 92, iss. 1, pp. 155–161. ISSN 0378-7796. DOI: 10.1016/j.epsr.2012.06.009.

[9] MESSALTI, S., S. BELKHIAT, S. SAADATE and D. FLIELLER. A New Approach for Load Flow Analysis of Integrated AC-DC Power systems using Sequential Modified Gauss-Seidel Methods. *European Transactions on Electrical Power*. 2012, vol. 22, iss. 4, pp. 421–432. ISSN 2050-7038. DOI: 10.1002/etep.570.

[10] WANG, W. and M. BARNES. Power Flow Algorithms for Multi-Terminal VSC-HVDC with Droop Control. *IEEE Transactions on Power Systems*. 2014, vol. 29, iss. 4, pp. 1721–1730. ISSN 0885-8950. DOI: 10.1109/TPWRS.2013.2294198.

[11] BEERTEN, J., S. COLE and R. BELMANS. Generalized Steady-State VSC MTDC Model for Sequential AC/DC Power Flow Algorithms. *IEEE Transactions on Power Systems*. 2012, vol. 37, iss. 2, pp. 821–829. ISSN 0885-8950. DOI: 10.1109/TPWRS.2011.2177867.

[12] KILIC, U. and K. AYAN. Optimizing Power Flow of AC-DC Power Systems using Artificial Bee Colony Algorithm. *International Journal of Electrical Power and Energy Systems*. 2013, vol. 53, iss. 1, pp. 592–602. ISSN 0142-0615. DOI: 10.1016/j.ijepes.2013.05.036.

[13] KILIC, U., K. AYAN and U. ARIFOGLU. Optimizing Reactive Power Flow of HVDC Systems using Genetic Algorithm. *International Journal of Electrical Power & Energy Systems*. 2014, vol. 55, iss. 1, pp. 1–12. ISSN 0142-0615. DOI: 10.1016/j.ijepes.2013.08.006.

[14] AYAN, K. and U. KILIC. Optimal Power Flow of Two-Terminal HVDC Systems using Backtracking Search Algorithm. *International Journal of Electrical Power & Energy Systems*. 2016, vol. 78, iss. 1, pp. 326–335. ISSN 0142-0615. DOI: 10.1016/j.ijepes.2015.11.071.

[15] ARAGGES-PENALBA, M., A. EGEA-ALVAREZ, O. GOMIS-BELLMUNT and A. SAMPER. Optimum Voltage Control for Loss Minimization in HVDC Multi-Terminal Transmission Systems for Large Offshore Wind Farms. *Electric Power Systems Research*. 2012, vol. 89, iss. 1, pp. 54–63. ISSN 0378-7796. DOI: 10.1016/j.epsr.2012.02.006.

[16] CALLE, I. A., P. LEDESMA and E. D. CASTRONUOVO. Advanced Application of Transient Stability Constrained-Optimal Power Flow to a Transmission System Including an HVDC-LCC Link. *IET Generation, Transmission & Distribution*. 2015, vol. 9, no. 13, pp. 1765–1772. ISSN 1751-8687. DOI: 10.1049/iet-gtd.2015.0215.

[17] RABIEE, A., A. SOROUDI and A. KEANE. Information Gap Decision Theory Based OPF with HVDC Connected Wind Farms. *IEEE Transactions on Power Systems*. 2015, vol. 30, iss. 6, pp. 3396–3406. ISSN 0885-8950. DOI: 10.1109/TPWRS.2014.2377201.

[18] SONG, H. M., M. H. SULAIMAN and M. R. MOHAMED. An Application of Grey Wolf Optimizer for Solving Combined Economic Emission Dispatch Problems. *International Review of Modelling and Simulations* 2014, vol. 7, no. 5, pp. 838–844. ISSN 1974-9821. DOI: 10.15866/iremos.v7i5.2799.

[19] MAHDAD, B. and K. SRAIRI. Blackout Risk Prevention in a Smart Grid based Flexible Optimal Strategy using Grey Wolf-Pattern Search Algorithms. *Energy Conversion and Management*. 2015, vol. 98, iss. 1, pp. 411–429. ISSN 0196-8904. DOI: 10.1016/j.enconman.2015.04.005.

[20] ESHA, G. and A. SAXENA. Robust Generation Control Strategy Based on Grey Wolf Optimizer. *Journal of Electrical Systems*. 2015, vol. 11, iss. 2, pp. 174–188. ISSN 1112-5209.

[21] SHAKARAMI, M. R. and I. F. DAVOUDKHANI. Wide-Area Power System Stabilizer Design based on Grey Wolf Optimization Algorithm Considering the Time Delay. *Electric Power Systems Research*. 2016, vol. 133, iss. 1, pp. 149–159. ISSN 0378-7796. DOI: 10.1016/j.epsr.2015.12.019.

[22] EL-FERGANY, A. and H. M. HASANIEN. Single and Multi-Objective Optimal Power Flow Using Grey Wolf Optimizer and Differential Evolution Algorithms. *Electric Power Components and Systems*. 2015, vol. 43, iss. 13, pp. 1548–1559. ISSN 1532-5008. DOI: 10.1080/15325008.2015.1041625.

[23] JAYAKUMAR, N., S. SUBRAMANIAN, S. GANESAN and E. B. ELANCHEZHIAN. Grey Wolf Optimization for Combined Heat and Power

Dispatch with Cogeneration Systems. *International Journal of Electrical Power & Energy Systems*. 2016, vol. 74, iss. 1, pp. 252–264. ISSN 0142-0615. DOI: 10.1016/j.ijepes.2015.07.031.

[24] GUHA, D., P. K. ROY and S. BANERJEE. Load Frequency Control of Interconnected Power System using Grey Wolf Optimization. *Swarm and Evolutionary Computation*. 2015, vol. 27, iss. 1, pp. 97–115. ISSN 2210-6502. DOI: 10.1016/j.swevo.2015.10.004.

[25] KAMBOJ, V. K., S. K. BATH and J. S. DHILLON. Solution of Non-Convex Economic Load Dispatch Problem using Grey Wolf Optimizer. *Neural Computing and Applications*. 2016, vol. 27, iss. 5, pp. 1301–1316. ISSN 0941-0643.

[26] SHARMA, Y. and L. C. SAIKIA. Automatic Generation Control of a Multi-Area ST - Thermal Power System using Grey Wolf Optimizer Algorithm based Classical Controllers. *International Journal of Electrical Power & Energy Systems*. 2015, vol. 73, iss. 1, pp. 853–862. ISSN 0142-0615. DOI: 10.1016/j.ijepes.2015.06.005.

[27] SHAKARAMI, M. R. and I. FARAJI. Design of SSSC-based Stabilizer to Damp Inter-Area Oscillations Using Gray Wolf Optimization Algorithm. In: *7th Electricity Power Generation Conference (EPGC)*. Bandar Abbas: CIVILICA, 2015, pp. 1–8.

[28] MIRJALILI, S., S. M. MIRJALILI and A. LEWIS. Grey Wolf Optimizer. *Advances in Engineering Software*. 2014, vol. 69, iss. 1, pp. 46–61. ISSN 0965-9978. DOI: 10.1016/j.advengsoft.2013.12.007.

[29] SAREMI, S., S. MIRJALILI and S. M. MIRJALILI. Evolutionary Population Dynamics and Grey Wolf Optimizer. *Neural Computing and Applications*. 2015, vol. 26, iss. 5, pp. 1257–1263. ISSN 0941-0643.

[30] MIRJALILI, S., S. SAREMI, S. M. MIRJALILI and L. S. COELHO. Multi-Objective Grey Wolf Optimizer: A Novel Algorithm for Multi-Criterion Optimization. *Expert Systems with Applications*. 2016, vol. 47, iss. 1, pp. 106–119. ISSN 0957-4174. DOI: 10.1016/j.eswa.2015.10.039.

[31] BEERTEN, J., S. COLE and R. BELMANS. Implementation Aspects of a Sequential AC/DC Power Flow Computation Algorithm for Multi-Terminal VSC HVDC Systems. In: *9th IET International Conference on AC and DC Power Transmission (ACDC)*. London: IET, 2010, pp. 1–6. ISBN 978-1-84919-308-5. DOI: 10.1049/cp.2010.1013.

About Authors

Heba Ahmed HASSAN received her B.Sc. and M.Sc. with Distinction First Honors degree from Electrical Power and Machines Department, Faculty of Engineering, Cairo University, Egypt, in 1995 and 1999, respectively. She obtained her Ph.D. degree in Electrical Engineering from the University of Ulster, UK, in 2004 when she was selected to present her Ph.D. work at the House of Commons, Parliament House, Westminster, London, UK. Dr. Hassan is a full-time faculty in Electrical Power and Machines Department, Cairo University, currently on leave. She joined Dhofar University, Sultanate of Oman in 2008 where she was promoted to several senior leadership positions. She was the Dean and Assistant Dean of College of Engineering, Dhofar University. She joined Oman Academic Accreditation Authority (OAAA) as Senior Quality Assurance Expert in October 2015. She was an Academic Visitor at the Imperial College, London, UK (1998), a Teaching and Research Assistant at the University of Ulster, UK (2001–2005), and a part-time faculty at many respectable private engineering universities in Egypt (2005–2008). During that period, she worked as a quality auditor for the Quality Assurance and Accreditation Project (QAAP) and a consultant for several Egyptian Ministry of Higher Education (MoHE) development projects financed by IBRD. She co-supervised master Students in Faculty of Engineering, Cairo University (2005–2012). Dr. Hassan was selected by reputable universities in India as an External Ph.D. Examiner and as a Keynote Speaker in several international conferences. She was appointed by the Omani MoHE as a Reviewer of newly submitted academic programs. Dr. Hassan is a Senior IEEE Member (SMIEEE), an IET Member (MIET), an Associate Fellow of the Higher Education Academy-UK (AFHEA) and a Certified Associate Academic Trainer by the International Board of Certified Trainers (IBCT). She is the Chief Editor of two international referred journals in the field. She is also serving as an Editorial Board Member and a Reviewer for many international journals and conferences in power engineering. Dr. Hassan research interests include electrical power systems stability and control, FACTS modeling, optimal and robust adaptive control and quality assurance of higher education.

Mohamed ZELLAGUI was born in Constantine, Algeria, in 1984. He received the engineering degree (Honors with first class) and M.Sc. degree in Electrical Engineering (Power System) from the Department of Electrical Engineering, University of Constantine, Algeria in 2007 and 2010, respectively. He received Doctor Degree in Power Systems from the Department of Electrical Engineering, University of Batna, Algeria in 2014. In 2012 obtained the national

award for the best Ph.D. student in science and technology. He has membership at International Association of Engineers (IAENG), Institute of Electrical and Electronics Engineers (IEEE), Power and Energy Society (PES), Smart Grid Community (SGC) and The Institute of Engineering and Technology (IET). He is a Senior Member of the Universal Association of Computer and Electronics Engineers (UACEE), International Scientific Academy of Engineering & Technology (ISAET) and International Association of Computer Science and Information Technology (IACSIT). His research interests include power systems protection, power electronics, renewable energy, FACTS devices and optimization techniques.